

The effect of the inhomogeneity of substrate on wetting transitions

H. Ez-Zahraouy*, L. Bahmad, and A. Benyoussef

Laboratoire de Magnétisme et de la Physique des Hautes Energies
Université Mohammed V, Faculté des Sciences, Avenue Ibn Batouta,
Rabat B.P. 1014, Morocco

Abstract

We study the substrate inhomogeneity effect on the wetting of a spin-1/2 Ising ferromagnetic film in an external magnetic field H , using Monte Carlo simulations. It is found the inhomogeneity leads to the formation of islands of positive spins in each layer. However, depending on the values of H , for a fixed surface magnetic field H_s , each layer exhibits three different phases; totally wet (TW), nonwet (NW) and partially wet (PW). In the latter case, we show the existence of three distinct configurations namely: A configuration (PWTD) in which the layer is partially wet with a total disconnection between islands; (PWPD) a configuration in which the layer is partially wet with a partial disconnection between islands; (PWTC) a configuration in which the layer is partially wet and the islands are totally connected. Furthermore, we show that an increase of H_s values breaks the bonds connecting some islands of the phase (PWTC) which leads to an expansion of the (PWPD) region. On the other hand, the frequency distribution and the average size of island are investigated in the (PWTD) region for fixed values of temperature T , H_s and H . Moreover, we show the existence of 3D-islands resulting from the formation of islands in each layer.

Keywords: Wetting; Monte Carlo simulations; Inhomogeneity; Layering; island distribution.

(*) Corresponding author: ezahamid@fsr.ac.ma

1 Introduction

Substantial research efforts have been devoted to the fabrication of quantum-dot structures, due to the interesting electronic and optical properties that can result from quantum confinement. Several novel applications for such structures have been envisaged such as the single-electron transistor and intersubband quantum-dot infrared photodetectors. The well studied technique of creating quantum dots is the use of *Si* deposition on *Ge* [1,2]. A significant number of studies have been performed with the aim of understanding the structural and compositional evolution of *Ge* islands growing. The role played by different growth parameters such as temperature, pressure and others have been studied for different growth techniques. The evolution of self assembled *Ge* islands in low pressure chemical vapor deposition of *Ge* on *Si*, using high growth rates, has been investigated by atomic force microscopy and Rutherford backscattering spectrometry [3].

On the other hand, the understanding of the nature and consequences of adsorbate-adsorbate interactions at solid surfaces is of great interest in engineering properties of interfacial materials. Many recent studies show that indirect interactions, mediated by the structure, can be significant enough to influence the formation of nano-structures at surfaces [4]. Indeed, much progress has been made recently in understanding adatom-pair interactions mediated by Shockley surface state electrons and the oscillatory interaction decays with adsorbate separation thickness [5-8]. Monte Carlo Simulations [9-11] and subsequently derived mean field theories [10,12], showed the existence of higher island densities than those expected by standard nucleation theory. It is shown that several experimental works, e.g. [8,13,14,15], supports these predictions, such as the deposition of *Au* on mica substrates at a high temperature [16-23].

In most cases, the electrical conductivity and practical utility of discontinuous metal films, have been extensively explored [24,25,26]. On the other hand, media that are magnetized perpendicular to the plane of the film, such as ultra thin cobalt films or multi layered structures [27,28], are more stable against thermal self-erasure [25,29] than conventional memory devices. In this context, magneto-optical memories seem particularly promising for ultrahigh-density recording on portable disks. The roughness and mobility of the magnetic domain walls [30,31] prevents closer packing of the magnetic bits, and therefore presents a challenge to reaching even higher bit densities. Increasing information storage to high densities may evolve through extensions

of current magnetic recording technologies. But such increases in storage density might be achieved by using other techniques such as holography, or micro machined nano-cantilever arrays [32]. The bit-writing with local probes may be thermally assisted by a current [33] or a laser beam that raises local temperature to the vicinity of the Curie temperature, resulting in the formation of a reversed domain with a rough wall. On the other hand, a strain implemented by a linear defect, in a magnetic thin film [34], can realize smooth and stable domain walls, that can be implemented without nano-scale patterning, Furthermore, composite materials such as multilayer coatings and isotropic nanocomposite coatings, having structures in the nanometer scale, can even show properties, which can not be obtained by a single coating material alone [35]. The most widely used coatings are TiN , TiC , $TiCN$, and combination thereof, as well as some coatings with lubricating properties such as diamond-like carbon. Monte Carlo simulations are applied to study the equilibrium magnetic domain structure of growing ultra thin ferromagnetic films with a realistic atomic structure [36]. Near the percolation threshold a metastable magnetic domain structure is obtained with an average domain area ranging between the area of individual magnetic islands and the area of the large domains observed for thicker ferromagnetic films. This micro-domain structure is controlled and stabilized by the non-uniform atomic nano-structure of the ultra-thin film, causing a random interaction between magnetic islands with varying sizes and shapes. The investigation of the magnetic domain formation, in nano-structured ultra-thin films, is an active field of current research. The influence of the atomic morphology on the magnetic properties is known to be especially strong during the initial states of the thin film growth. A small variation of the preparation conditions may considerably change the obtained magnetic structure. This has been shown, by resolving imaging techniques, which allows the investigation of atomic structure as well as the magnetic domain structure of several nanostructured systems [37-42].

Our aim in this work is to study the effect of the inhomogeneity of substrate on the wetting transitions of a spin-1/2 Ising film when a surface magnetic field is applied on alternate clusters of the surface. The case of a uniform surface magnetic field has been considered in one of our previous works [43]. The geometry effect under the presence of an edge was subject of our work presented in Ref. [44].

The paper is organized as follows. In section 2, we describe the model and the method used: Monte Carlo (MC) simulations. In section 3 we present results and discussions.

2 Model and Monte Carlo simulations

The system we are studying, illustrated by Fig. 1, is a magnetic thin film formed with $N = 4$ layers coupled ferromagnetically. Each layer is a square of dimension $N_x \times N_y = 64 \times 64$ spins. N_x and N_y stand for the number of spins in the x and y directions, receptively. A surface magnetic field H_s is acting only on alternate clusters of spins of the surface $k = 1$. This is represented, in Fig. 1, by symbols (+) for alternate clusters of dimension $l_p \times l_p = 8 \times 8$. Whereas H_s is absent for the remaining alternate clusters of dimension $l_n \times l_n = 8 \times 8$. These clusters are represented by symbols (o). l_p (resp. l_n) denotes The size of alternate clusters , receptively.

The Hamiltonian governing this system is given by

$$\mathcal{H} = -J \sum_{\langle i,j \rangle} S_i S_j - \sum_i (H + H_{s_i}) S_i \quad (1)$$

where, $S_i (i = i, j) = -1, +1$ are the spin variables and the interaction between different spins is assumed to be constant. The surface magnetic field H_{s_i} applied on each site i of the surface $k = 1$, is distributed alternatively, so that:

$$H_{s_i} = \begin{cases} +H_s & \text{for all sites } i \in \text{clusters with symbols (+)} \\ 0 & \text{for all sites } i \in \text{clusters with symbols (o)}. \end{cases} \quad (2)$$

H is an external magnetic field applied on each layer of the system.

We perform Monte Carlo simulations under the Metropolis algorithm, a preliminary study showed that the relevant calculated quantities did not change appreciably when the film thickness varies from $N = 3$, $N = 4$, $N = 5$ to $N = 8$ layers and when varying the number of spins of each layer from $N_x = N_y = 32$ to 128; where N_x and N_y are the number, of spins of each layer, in the x and y -directions, respectively. Taking into account the above considerations, in the following numerical results will be given for a film with $N = 4$ layers and $N_x = N_y = 64$ spins for each layer.

3 Results and discussion

A sketch of the geometry of the system we are studying, is presented in Fig. 1. The film is formed by $N = 4$ layers. In order to outline the phenomenon of increasing islands, for negative spins of the surface $k = 1$, we plot in Fig. 2, the island size as well as the number of islands of negative spins. Indeed, for $H_s = 2.5$ a temperature $T = 3.5$, starting from $H = 0$ and decreasing the external magnetic field H , two islands occur for $H \approx -0.1$, with increasing number of negative spins. For $H < -0.15$, the number of islands increases rapidly, and mean island size undergoes a local maximum. When decreasing the magnetic field H more and more, $H < -0.20$ the number of clusters stabilizes at 32 corresponding to a mean size island value 64. For $H \approx -0.80$ the different clusters of negative spins are connected to each other to form a unique island. On the other hand, the increasing surface magnetic field effect, on island formation of negative spins, is illustrated by Figs. 3a and 3b for a fixed temperature $T = 3.5$ for several values of the surface magnetic field: $H = 1.5$, $H = 2.0$ and $H = 2.5$. Indeed, for small values of the magnetic field, $H > -0.20$, the increasing surface magnetic field is not felt at this "higher" temperature value 3.5. While, for $H < -0.20$, the increasing surface magnetic field amplitude is to produce a large step of mean size island value 64, see Fig. 3a. It is worth to note that this step disappears for very small surface magnetic field values. Concerning the number of negative spin islands, the same arguments still valid when increasing the surface magnetic field amplitude H_s , Fig. 3b. The islands are rapidly connected to each other for very small values of H_s . On the other hand, depending on the values of H , we show the existence of three regions, of island configurations of positive spins in the plane (T, H) , for a fixed surface magnetic field H_s . These three different regions, in the phase diagram (T, H) , are; a totally wet (TW) region, a nonwet (NW) region and partially wet region. In this latter case, we show the existence of three distinct island configurations of positive spins, namely; the (PWTD) configurations where the layer is partially wet with a total disconnection of the islands; the (PWPD) configurations in which the layer is partially wet with a partial disconnection of the islands; The (PWTC) configurations corresponding to a partially wet layer with totally connected islands of positive spins are.

Indeed, Fig. 4, summarizes these regions for the layer $k = 4$, with several values of the surface magnetic field H_s : 1.5; 2.0 and 2.5. It is worth to note that at low temperature values, only the totally wet (TW) phase, and the non wet (NW) phase are present, depending on the

value of the external magnetic field H . At higher temperature values, provided that T is kept less than the critical value $T_c = 3.87$, the partially wet phase is found. Indeed, an increasing amplitude of the external magnetic field H (from 0 negative values), give rise to the partially wet phase (PWTC) in which the islands are totally connected, followed by the phase (PWPD) with configuration of islands partially disconnected. Increasing more the magnetic field H values, the phase (PWTD) is reached showing totally disconnected configuration of islands. Increasing more and more the magnetic field H , the totally wet phase (TW) is reached and persists when $H \rightarrow \infty$.

The Fig. 4 shows also that increasing values of Hs breaks the bonds of the partially connected islands of the phase (PWPD), so that the limit (PWPD)/(PWTD) regions is displaced towards the (PWTD) region. The temperature corresponding to Fig. 4. is not sufficient to overcome the bonds connecting the islands of the (PWTC) region. Hence, the limit (PWPD)/(PWTD) is kept constant.

To more clarify these findings, we plot in Figs. 5a and 5b, different island positive spin configurations in different regions of the phase diagram for each layer. Indeed, Fig. 5a, shows that, for $Hs = 2.0$, $T = 3.5$ and $H = -0.13$, the first layer $k = 1$ is in the (PWTC) configuration, the second layer $k = 2$ is in the (PWPD) configuration, whereas the third layer $k = 3$ is in the (PWTD) phase. On the other hand, when maintaining the parameters T and Hs constant, and varying only the external magnetic field, a given layer undergoes different configurations belonging to different regions: (PWTC), (PWPD) and (PWTD). This situation is illustrated by Fig. 5b for the last layer $k = 4$. Indeed, for $H = -0.13$ this layer is in the region (PWTC), for $H = -0.15$ the configuration of (PWPD) region is present; and when $H = -0.17$ the islands of this layers are completely disconnected from each other so that this configuration belongs to (PWTD) region. Moreover, the formation of islands in each layer leads to the formation the three dimensional islands ($3D$ -islands). Indeed the superposition of the $2D$ -island of adjacent layers give rise to the appearance of such $3D$ -islands in the film. For example, Fig.5a shows this $3D$ -island, when superposing the layers over each other. One can note this situation, for example, for the rectangle of coordinates in the rectangle $16 \geq x \geq 24$ and $32 \geq y \geq 40$ for the layers $k = 1, 2, 3$ and 4 respectively. The superposition of these islands constitute a three dimensional island in the bulk of the film. However, the height of the formed island depends on the values of temperature, surface and external magnetic fields. In the example of Fig. 5a,

the island height is close to 4. A preliminary study showed that the island height decreases with decreasing values of H_s , for fixed values of temperature T and external magnetic field H . In order to illustrate the frequency distribution of different configurations, we plot in Fig. 6 the corresponding frequency island size distributions, in the (PWTD) region, for the layers $k = 1$, $k = 2$, $k = 3$ and $k = 4$ for a temperature $T = 3.5$, $H_s = 2.0$ and $H = -0.142$. The different scenarios presented by the system concerning the inhomogeneity substrate effect on the distribution of island sizes and number of existing islands are presented. Indeed, the mean size islands of negative spins undergoes a local maximum before exhibiting a first and second steps. The plateau of the first step increases with increasing surface magnetic field values.

4 Conclusion

We have studied the effect of the inhomogeneity of a substrate on the wetting transitions of a spin-1/2 ferromagnetic Ising thin film under the effect of an alternate surface magnetic field H_s acting on alternate islands of the surface, using Monte Carlo simulations. In the partial wetting region each layer exhibits three different configurations namely: partial wetting with totally disconnected island (PWTD), partial wetting with partially disconnected islands (PWPD) and partial wetting with totally connected islands (PWTC) On the other hand, we found that increasing the surface magnetic field leads to the disconnection of some connected islands in the (PWPD) region. Furthermore the 3D-islands occur for strong surface magnetic field. Moreover, the distributions of the islands size, in each layer of the film, are also computed.

References

- [1] R. Hull and J. C. Bean (Eds) *Semicond. semicond.* **56** (1999).
- [2] E. Kasper and K. Lyutovich in '*Properties of Silicon Germanium and SiGe: Carbon*, EMIS Datareviews Series **24** (INSPEC, IEE, London, 2000).
- [3] G. D. M. Dilliwai, D. M. Bagnall, N. E. B. Cowern and C. Jeynes, *J. Mat. Sci.: Mat. in Elect.* **14**, 323 (2003)
- [4] K. A. Fichthorn and M. L. Merrick, *Phys. Rev. B* **68**, 041404 (R) (2003).

- [5] K. Lau and W. Kohn Surf. Sci. **65**, 607, (1977).
- [6] P. Hyldgaard and M. Persson J. Phys.: Condens. Matter **12**, L13, (2000).
- [7] K. A. Fichthorn and M. Scheffler, Phys. Rev. Lett. **84**, 5371, (2000).
- [8] N. Knorr, H. Brune, M. Epple, A. Hirstein, M. A. Shneider and K. Kern, Phys. Rev. B **65**, 115420, (2002).
- [9] S. Ovesson, A. Bogicevic, G. Wahnstrom, and B. I. Lundqvist, Phys. Rev. B **64**, 115423, (2001).
- [10] S. Ovesson, Phys. Rev. Lett. **88**, 116102, (2002).
- [11] K. A. Fichthorn, M. L. Merrick, and M. Scheffler, Appl. Phys. A: Mater. Sci. Process. **75**, 17, (2002).
- [12] J. A. Venables and W. Kohn Phys. Rev. B **66**, 195404, (2002).
- [13] H. Brune, K. Bromann, K. Kern, J. Jacobsen, P. Stolze, K. Jacobsen, and J. Norskov, Phys. Rev. B **52**, R14 380, (1995).
- [14] J. V. Barth, H. Brune, B Fischer, J. Weckesser, and M. Scheffler, Comput. Phys. Commun. **107**, 187, (1997).
- [15] X. Y. Zheng, Y. Ding, L. A. Bottomley, D. P. Alison, and R. J. Warmack, J. Vac. Sci. Technol. B **13**(3), 187, (1995).
- [16] K. Reichelt and H. O. Lutz, J. Cryst. Growth **10**, 103, (1971).
- [17] C. E. D. Chidsey, D. N. Loiacono, T. Sleator, and S. Nakahara, Surf. Sci. **200**, 45 (1988).
- [18] A. Putnam, B. L. Blackford, M. H. Jericho, and M. O. Watanabe Surf. Sci. **217**, 276 (1989).
- [19] J. A. DeRose, T. Thundat, L. A. Nagahara, and S. M. Lindsay, Surf. Sci. **256**, 102 (1991).
- [20] R. Koch, D. Winau, A. Fuhrmann, and K. H. Reider, Vacuum **43**, 521 (1992).

- [21] M. Hegner, P Wagner, and G. Semenza, Surf. Sci. **291**, 39 (1993).
- [22] J. E. Morris and T. J. Coutts, Thin Solid Films **47**, 3 (1977).
- [23] P. G. Borziak, Y. A. Kulyupin, S. A. Nepijko, and V. G. Shamonya, Thin Solid Films **76**, 359 (1981).
- [24] *Magnetic Recording: The First Hundred Years*. Eds. Daniel, E.D. Mee, C.D. and Clark, M. H. (IEEE Press, New York, 1998).
- [25] D. A. Thompson and J. S. Best, IBM J. Res. Develop. **44**, 311 (200)
- [26] A. Hubert and R. Schafer, *Magnetic Domains*. (Springer, New York, 1998).
- [27] R. D. Kirby, J. X. Shen, R. J. Hardy, and D.J. Sellmyer, Phys. Rev. B **65**, R10 810, (1994).
- [28] R. Allenspach, M. Stampanoni, and A. Bischof, Phys. Rev. Lett. **65**, 3344 (1990).
- [29] D. Weller and A. Moser, IEEE Trans. Magn. **35**, 4423, (1999).
- [30] S. K. Han, S.-C. Yu, and K. V. Rao, J. Appl. Phys. **79**, 4260 (1996).
- [31] S. Lemerle, J. Ferre, C. Chappert, V. Mathet, T. Giamarchi, and P. Le Doussal, Phys. Rev. Lett. **80**, 849 (1998)
- [32] J. F. Heanue, M. C. Bashaw, and L. Hasselink, *Science* **265**, 749 (1994).
- [33] J. Nakamura, M. Miyamoto, S. Hosaka, and H. Koyanagi, J. Appl. Phys. **77**, 779 (1995).
- [34] L. Krusin-Elbaum, T. Shibauchi, B. Argyle, L. Gignac, and D. Weller *Nature* **410**, 444 (2001)
- [35] R. Hauert and J. Patscheider, Adv. Eng. Mater. **2** No. 5, 247 (2000).
- [36] R. Brinzanik, P. J. Jensen, and K. H. Bennemann, J. Magn. Mater. **238** 258 (2002).
- [37] R. Allenspach, M. Stampanoni, and A. Bischof, Phys. Rev. Lett. **65**, 3344 (1990).
- [38] R. Allenspach, J. Magn. Mater. **129**, 160 (1994).

- [39] H. P. Oepen, M. Speckmann, Y. Millev, and J. Kirschner , Phys. Rev. B **55**, 2752 (1997).
- [40] E. Mentz, A. Bauer, D. Weiss, and G. Kaindl, Matter. Res. Soc. Symp. **475**, 431 (1997).
- [41] W. Kuch, J. Gilles, S. S. Kang, S. Imada, S. Suga, and J. Kirschner, Phys. Rev. B **62**, 3824 (2000).
- [42] A. Kubetzka, O. Pietzsch, M. Bode, and R. Wiesendanger , Phys. Rev. B **63**, 140407(R) (2001).
- [43] A, Benyoussef, H. Ez-Zahraouy, Physica A **206**, 196(1994); *ibid*, J. Phys. I France 4, 393 (1994)
- [44] L. Bahmad, A, Benyoussef, and H. Ez-Zahraouy, Phys. Rev. E **66**, 056117 (2002); *ibid*, M. J. Condensed Matter **4**, 84 (2001)

Figure Captions

Figure 1.:

A geometry sketch of the studied system formed with $N = 4$ layers. A surface magnetic field H_s is acting on alternate island spins of the surface $k = 1$. H_s is present on islands with symbols: '+', and absent elsewhere: islands with symbols 'o'.

Figure 2:

The dependency of the mean island size, and the number of islands of the surface $k = 1$ for negative spins, as a function of the external magnetic field H for a fixed temperature $T = 3.5$ and a surface magnetic field value $H_s = 2.5$.

Figure 3:

- (a) The surface mean size island as a function of H .
- (b) The number of islands of negative spins in the surface as a function of H for $T = 3.5$ and several values of H_s : 1.5; 2.0 2.5.

Figure 4:

The (T, H) phase diagram for the layer $k = 4$, as a function of the external magnetic field H ,

for several values of the surface magnetic field H_s : 1.5; 2.0 and 2.5.

Figure 5:

island maps of positive spins for different layers of the film with $N = 4$ a) The first layer $k = 1$ is in the (PWTC) configuration, the second layer $k = 2$ is in the configuration (PWPD), while the layer $k = 3$ belongs to the configuration (PWTD); for $T = 3.5$, $H = -0.13$ and $H_s = 2.0$. b) For $H = -0.13$, $H = -0.15$ and $H = -0.17$, the last layer $k = 4$ exhibits three different configurations (PWTC), (PWTD) and (PWTD), respectively, for $T = 3.7$ and $H_s = 2.0$.

Figure 6:

Frequency island size distributions for the layers $k = 1$, $k = 2$, $k = 3$ and $k = 4$ for the configuration (PWTD) corresponding to $T = 3.5$, $H_s = 2.0$ and $H = -0.142$.

Fig. 1

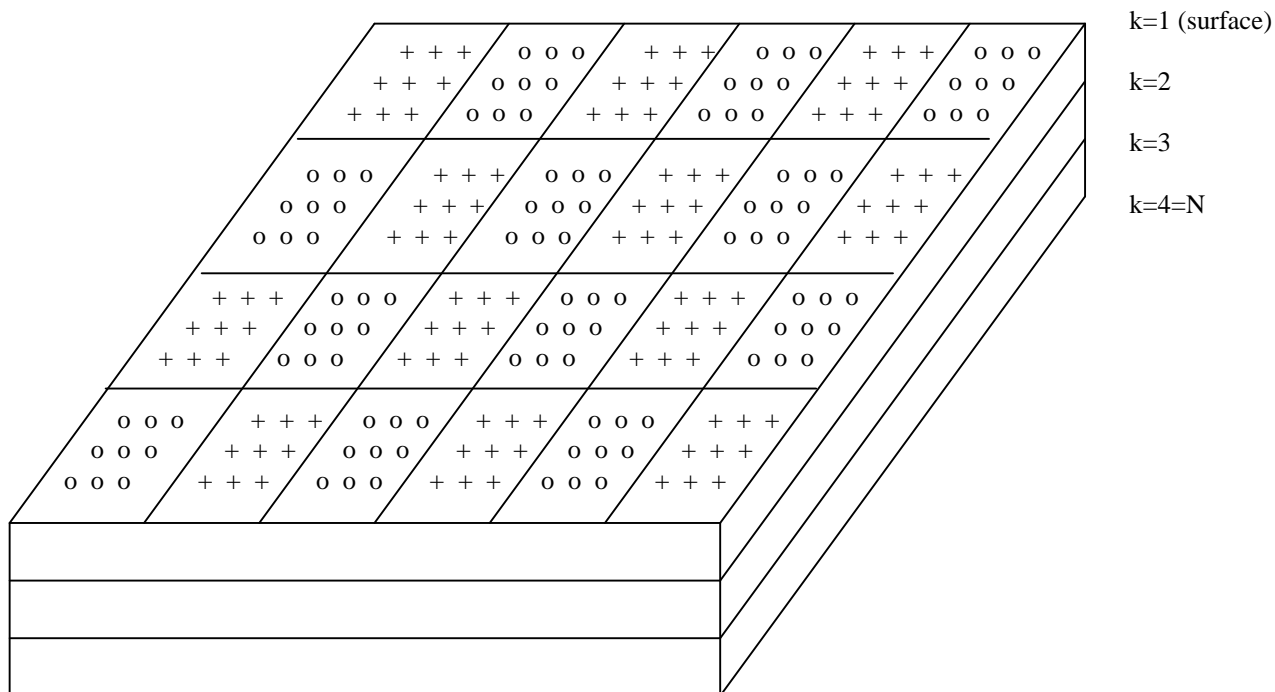


Fig. 2

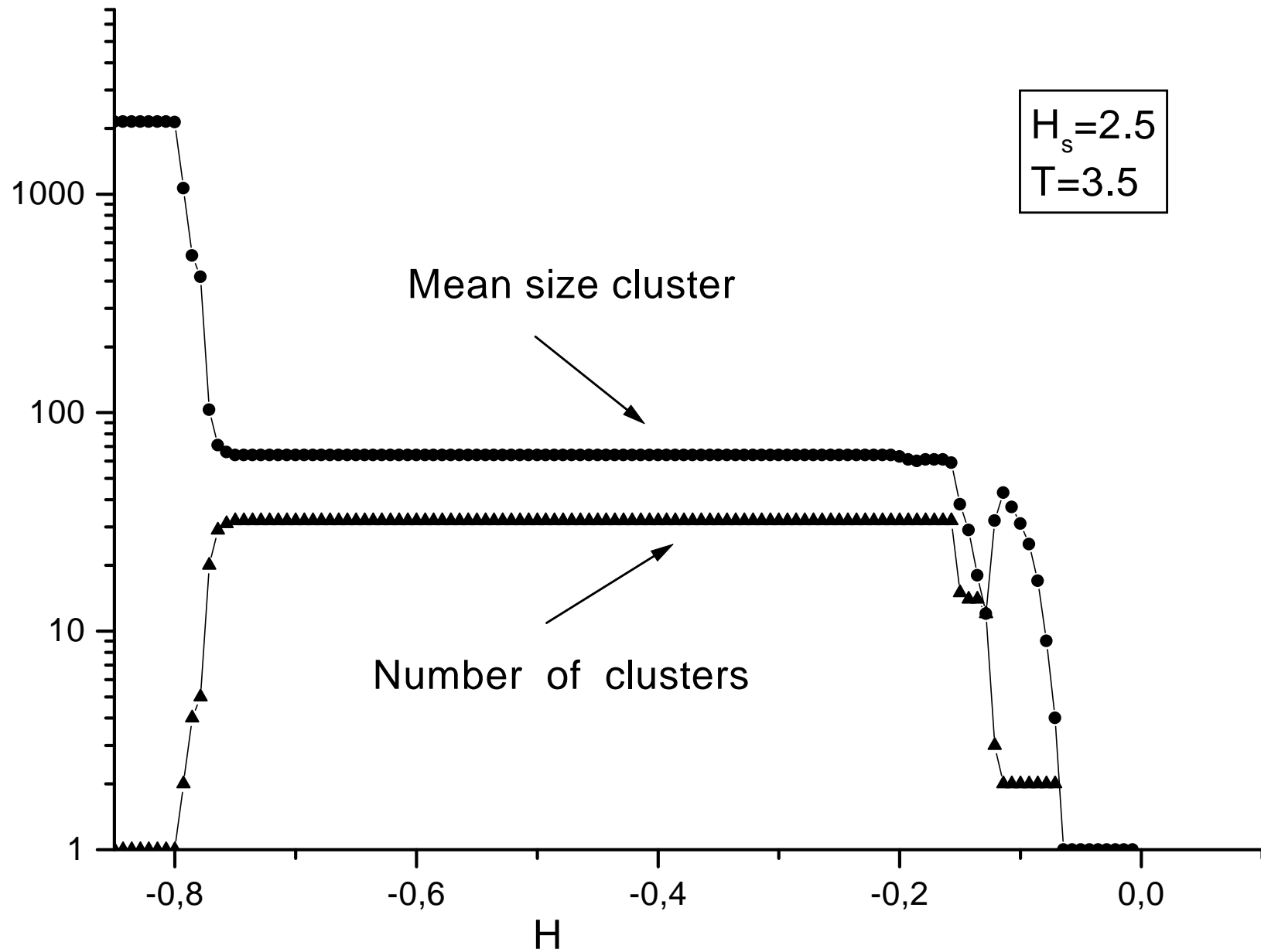


Fig. 3a

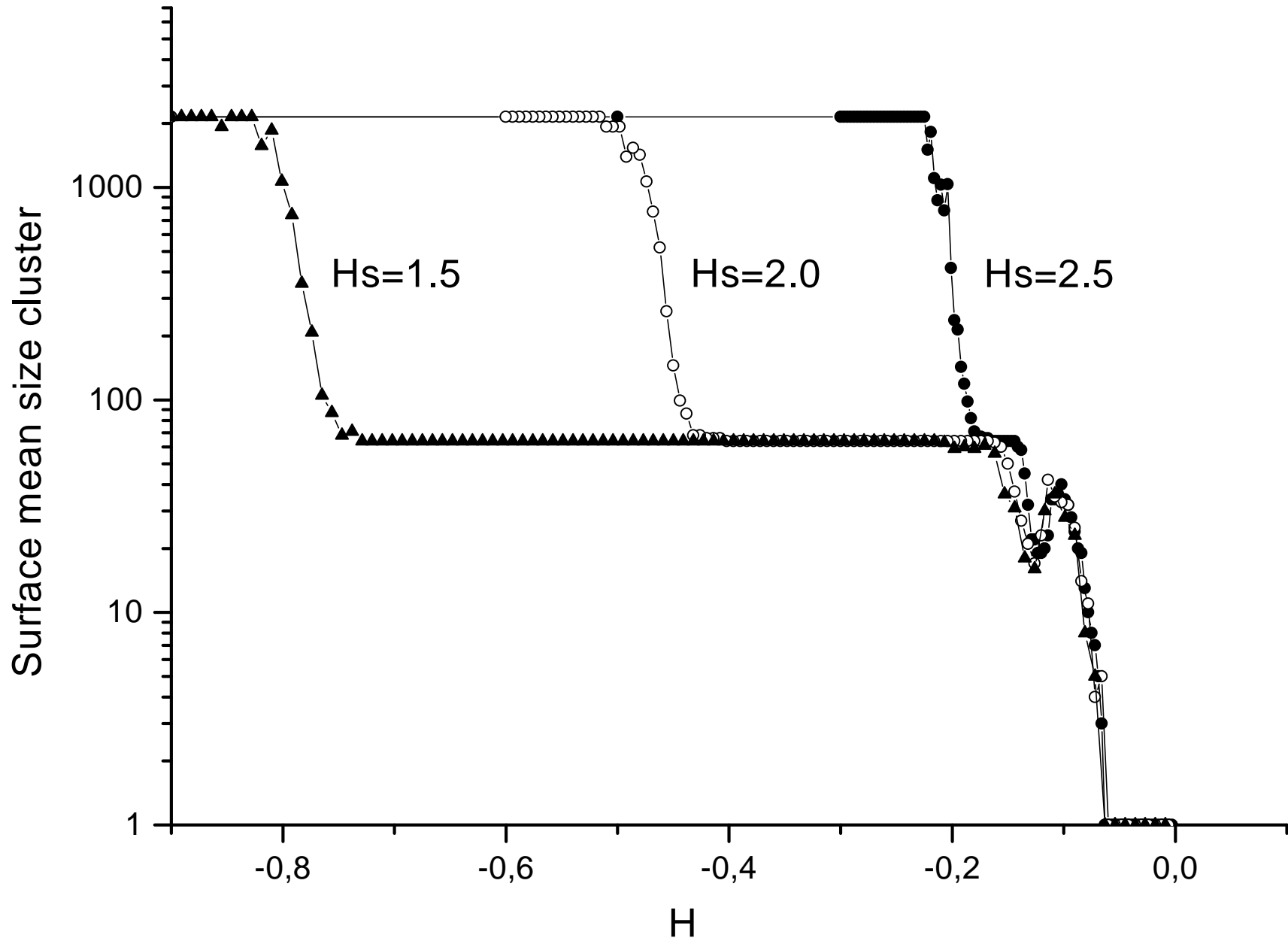


Fig. 3b

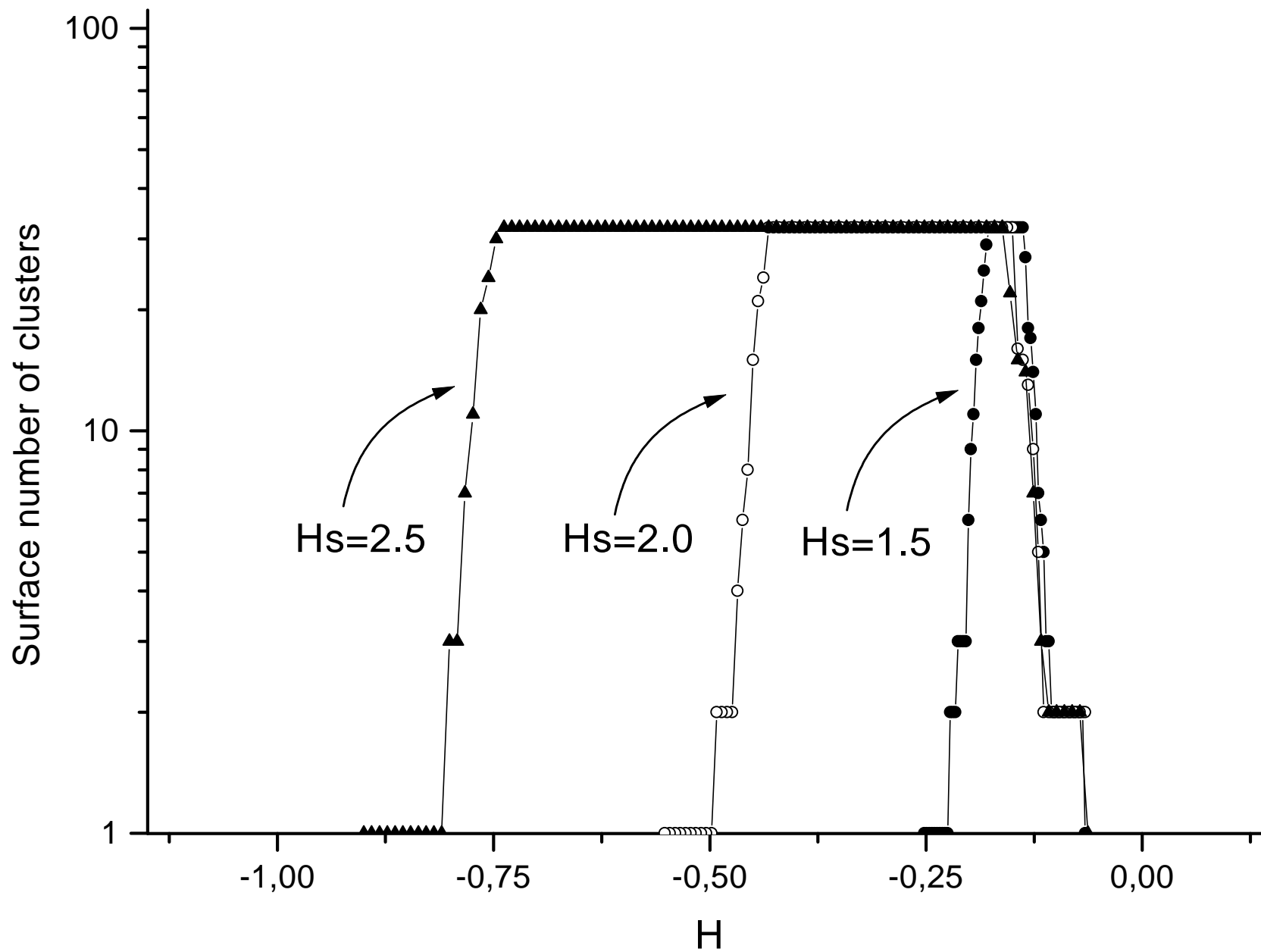


Fig. 4

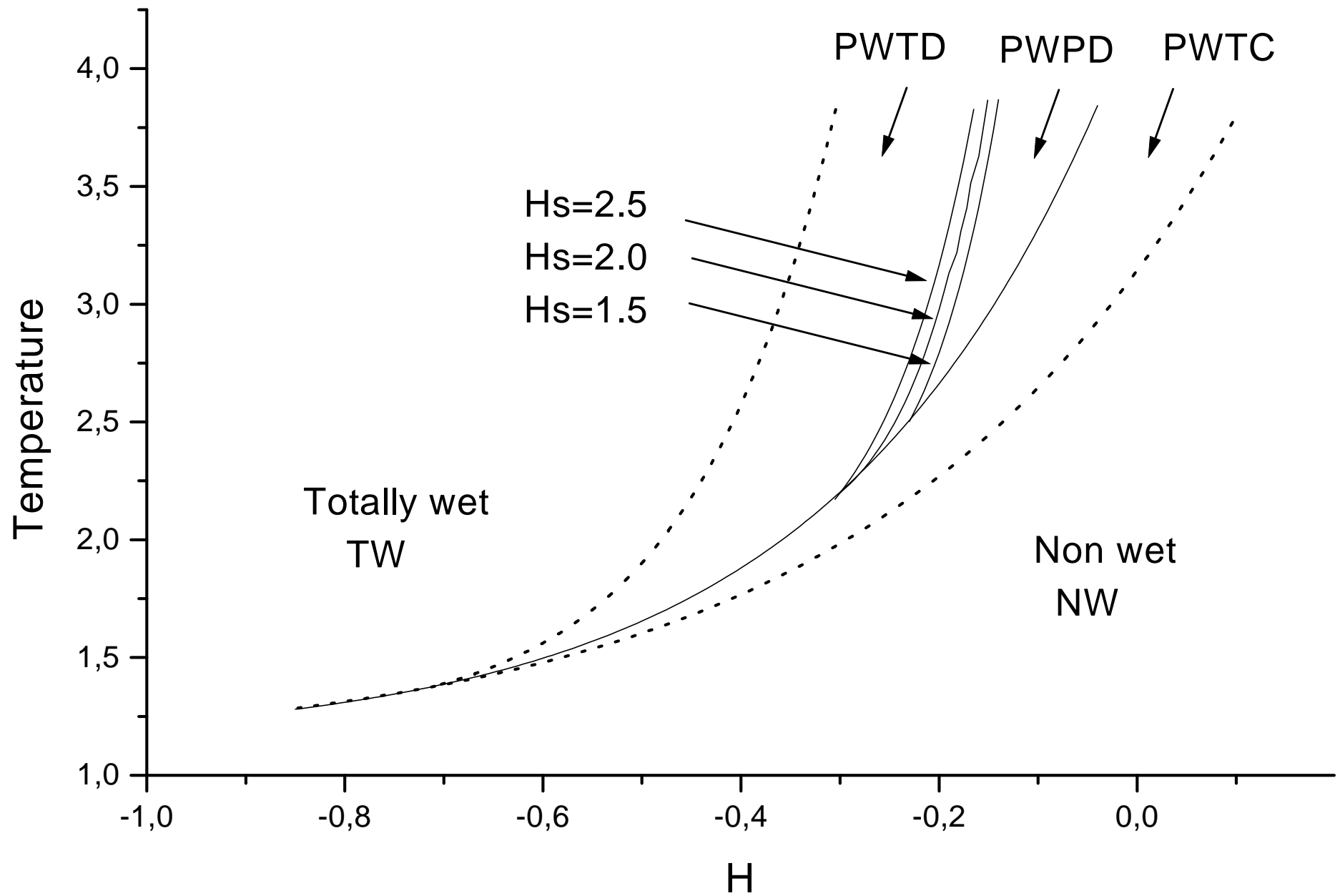
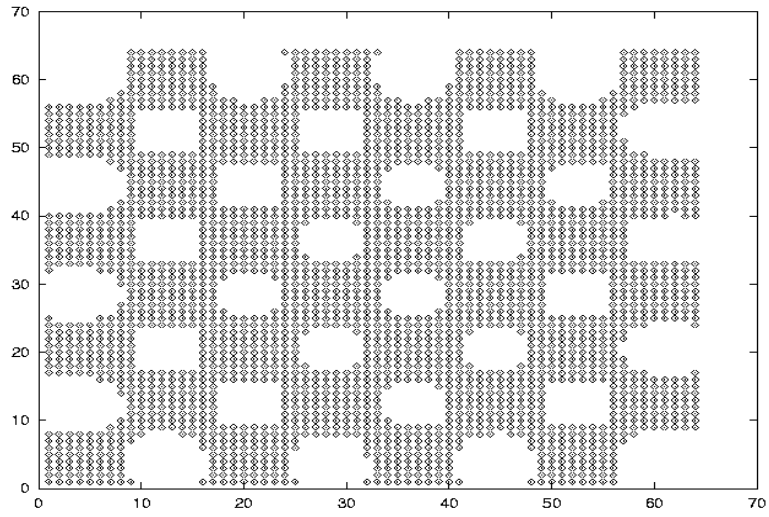
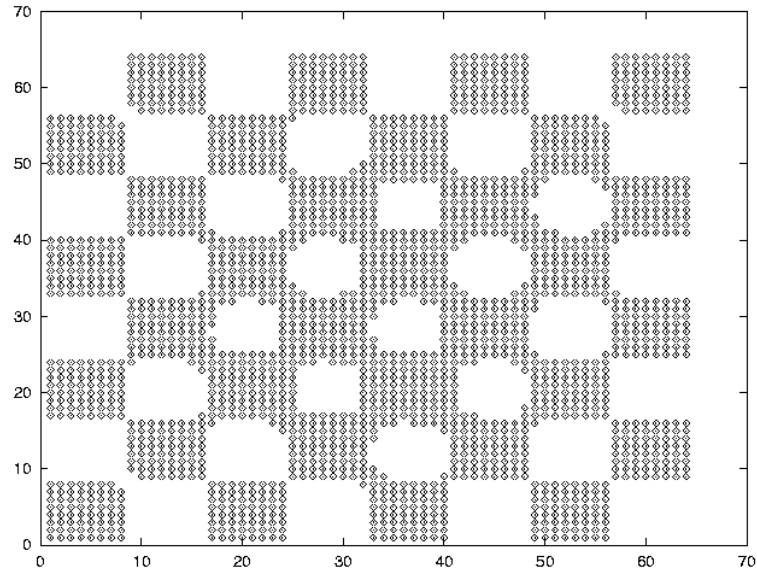


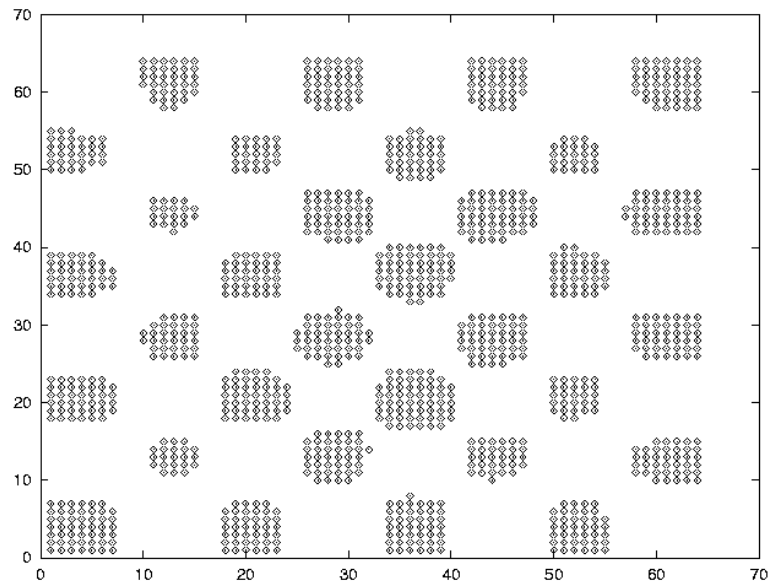
Fig. 5a



k=1
PWTC

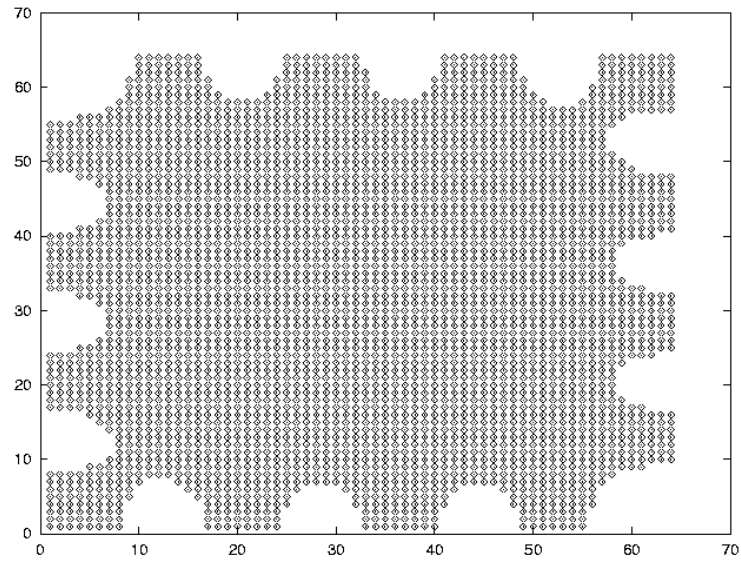


k=2
PWPD

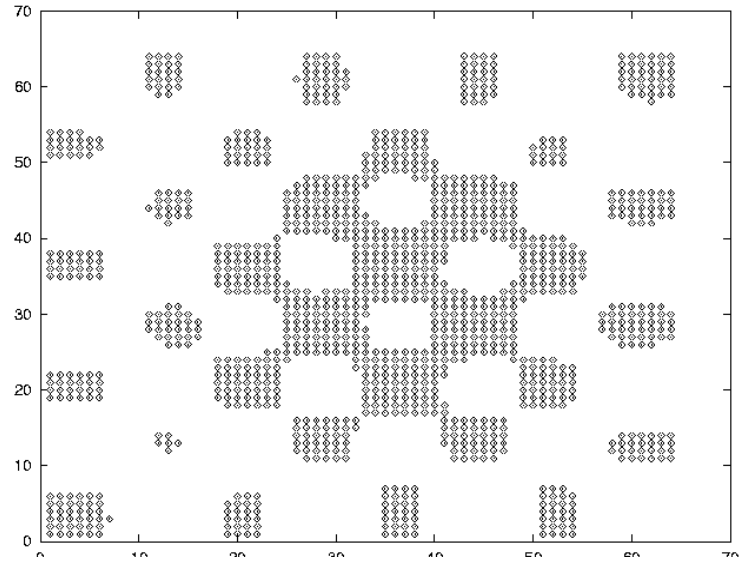


k=3
PWTB

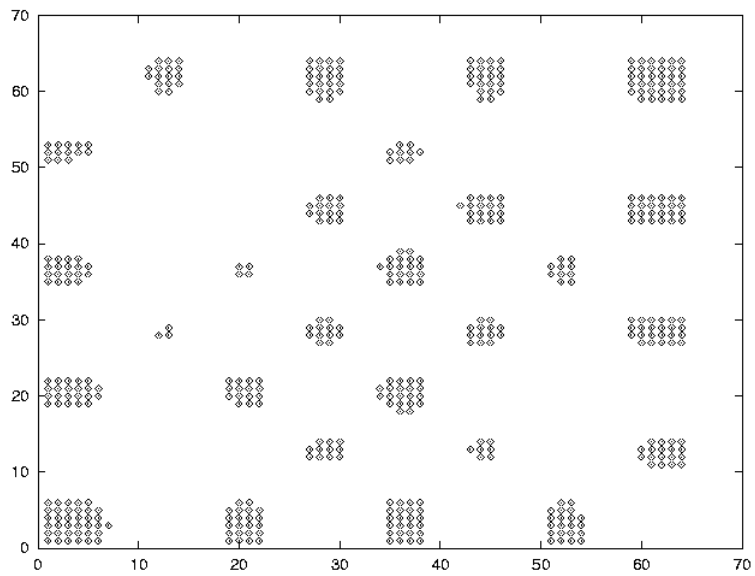
Fig.5b



k=4
PWTC



k=4
PWPD



k=4
PWTD

Fig. 6

